Experimental study of the cooling performance of phase change material with discrete heat sources – Continuous and intermittent regimes

Salma Gharbi, Souad Harmand, Sadok Ben Jabrallah

Applied Thermal Engineering 111 (2017) 103–111

Experimental study of the cooling performance of phase change material with discrete heat sources – Continuous and intermittent regimes

Salma Gharbi [a,*], Souad Harmand [b], Sadok Ben Jabrallah [a]

[a] University of Carthage, Science Faculty of Bizerte, 7021 Bizerte, Tunisia
[b] University Lille Nord de France, F-59000 Lille, UVHC, LAMIH, F-59313 Valenciennes, France

Highlights

- Study on thermal performance of PCM with three discrete heat sources.
- Examination of heat transfer mechanism for different heat flux repartition between sources.
- An intermittent regime is investigated for different heat flux cycle.
- An extended critical time is shown when the greater part of heat flux is placed at middle or lower source.
- Fractionating cycle length into 4 or 8 cycles can keep plate temperature under critical condition for longer time.

Keywords:
Phase change material
Discrete heat sources
Electronic cooling
Heat transfer
Melting
Intermittent regime

Abstract

This paper presents an experimental investigation of phase change material (PCM, Plastic paraffin) behavior in a rectangular enclosure with three discrete heat sources flush-mounted on the right vertical wall. The remaining walls of the cavity are adiabatic. Maximizing the critical time (time required by one of the electronic components before reaching the critical temperature) is the global objective of this study. Conserving constant the total flux, the thermal performance of system is examined by different heat flux repartition between sources. Also, the intermittent regime is studied for different heat flux cycle. The results show that the thermal performance depends strongly on the heat flux repartition and the maximum heat transfer is seen for the lower source. Placing the greater part of heat flux at middle or lower source seems the best manner to extend the critical time. For intermittent regime, it is concluded that fractionating cycle length into 4 or 8 cycles can keep plate temperature under critical condition for respectively 3 and 5 times comparing to one cycle.

1. Introduction

With the progress of electronic devices development, they become more and more potential site of high power. Therefore, thermal control become an extremely challenge for electronic equipment safety and reliability. The major objective of interest for the cooling is maintaining the component temperature below a maximum limit.

In recent years, using PCMs for electronic cooling presents a promising technique. By absorbing the heat generated by components it offer a relatively large period of temperature stabilization. Kandasamy et al. [1] studied numerically and experimentally the use of PCM (Paraffin wax) based heat sink for thermal management of portable electronic devices under cyclic steady conditions. It was concluded that using PCM-based heat sinks improve the thermal performance of electronic component during intermittent use. For cooling portable hand held electronic devices, Tan and Tso [2] investigated experimentally a heat storage unit filled by PCM (n-eicosane). They reported that the use of PCM can stabilize the temperature system and extend the operation time. Faraji and El Qarnia [3] analyzed numerically cooling of microprocessors using a PCM heat sink in a cyclic operating mode. It was found that the established periodic mode was reached after three cycles of working. Gharbi et al. [4] conducted an experimental analysis of different configurations of heat sink based PCM (Plastic paraffin). The results indicated that the inclusion of PCM can lower component increase temperature and the combination of PCM and long, well-spaced fins presents an effective means for thermal control of electronic devices.

In most applications, multiple components dissipate heat mutually and periodically during the operating period. Therefore,

* Corresponding author.
E-mail address: sallema0208@live.com (S. Gharbi).

DOI : 10.1016/j.applthermaleng.2016.06.109

Nomenclature

C_p	specific heat capacity, kJ kg^{-1} K^{-1}
F	amplitude
g	gravitational constant, m s^{-1}
H_l	liquid fraction
H	heat source
k	thermal conductivity, W m^{-1} K^{-1}
L_m	melting heat, kJ kg^{-1}
PCM	phase change material
P	pressure, N m^{-2}
Q	heat flux, W m^{-2}
T	temperature, °C
t	time, s
U, V	velocities, m s^{-1}
ρ	density, kg m^{-3}
μ	dynamic viscosity, Pa s
β	volumetric expansion coefficient, (1/K)
amb	ambient
c	critical
eq	equivalent
0	reference
1, 2, 3	upper, middle and lower heat source
gr	great part of heat flux
l	liquid
m	melting
w	weak part of heat flux
s	solid

cooling discrete sources have received a great interest by many authors. Keyhani et al. [5] performed an experimental study on natural convection heat transfer in a tall vertical rectangular enclosure with an array of eleven discrete heaters. It was showed that compared to the uniformly heated vertical wall, the discrete heating in the cavity augments more the local heat transfer rate. Chadwick et al. [6] have experimentally and theoretically investigated the heat transfer in a rectangular enclosure for single and multiple heaters attached on one vertical wall. It was revealed that for single and dual heaters, the higher heat transfer corresponds to the bottom heater location in the high Grashof number range. The optimum spacing problem was investigated by Liu and Phan-Thien [7]. For three heated chips mounted on a conductive substrate in a two-dimensional rectangular enclosure filled with air, the optimum thermal performance was found when the center-to-center distances between the chips follows a geometric series (the geometric ratio is the golden mean 1.618). More recently, in order to maximize the global conductance in enclosure, Kadiyala and Chattopadhyay [8] performed an optimization of location of heat sources in a vertical square enclosure with natural convection. The results showed that the optimal location of the three heat sources should be as close as possible to the bottom adiabatic wall.

Numerous studies have been performed on heat transfer in cavity discretely heated from below: Deng et al. [9] investigated numerically the interaction between two discrete flush-mounted heat sources at the bottom of an enclosure with insulating side walls. They examined the effects of the Rayleigh number, the thermal strength, and the separation distance on the interaction between sources. The result showed that the lowest maximum temperature is noted when the distance between sources is nearly close to height. Basak et al. [10] studied numerically laminar natural convection flow in a square cavity with uniformly and non-uniformly heated single bottom wall and adiabatic top wall. It was concluded that the sinusoidal nonuniform heating improves the heat transfer rates at the center of the bottom wall than the uniform heating case for all Rayleigh numbers.

Thanks to its high removal heat and energy storage density, using PCM may be a promising alternative for cooling multiple operating components. Research by Binet [11] developed a mathematical model (2D) of the thermal behavior of PCM (octadecane) inside a vertical rectangular cavity with three discrete heat sources. It was reported that cavities with a high aspect ratio (>4) show better thermal control of the heat sources and provide relatively long melting times. Yuwen et al. [12] conducted an experimental study on the melting process of the n-octadecane in a rectangular cavity with three protruding discrete heat sources. The effects of Stefan number, the sub-cooling and aspect ratio on the melting process were analyzed. It was concluded that the upper source has the higher temperature and subcooling weakens natural convection. Zhang et al. [13] studied analytically the melting of the PCM (n-octadecane) within a rectangular cavity heated by three sources flush-mounted on one of its vertical walls with adiabatic other walls. They evaluated the effect of heat source dimension and the conductivity of unheated part on thermal performance. The results obtained show that increasing heat source dimension reduces the surface source temperature. Also, with the increase of unheated part conductivity the upper source temperature rises while that of lower source decreases.

Faraji et al. [14] developed a 2D mathematical model in order to explore the behavior and the thermal performance of a vertical rectangular enclosure filled with PCM (n-eicosane) heated by three heat sources attached to a vertical wall. They concluded that the maximum temperature is at the central source when conduction is dominant, while the upper heat source stores this maximum temperature when the convection develops. The highest rate of heat transfer is observed for the lower heat source. El Qarnia et al. [15] performed a numerical study on the melting of PCM (n-eicosane) in a rectangular cavity heated by three heat sources mounted on a vertical conductive plate. They examined the effect of different parameters such as Rayleigh number and the inter-unit spacing on the thermal performance. The results indicate that the critical time is reduced by increasing the spacing between sources and the lower position of the sources shows the best cooling. Mirzaei et al. [16] studied numerically the melting of PCM (Paraffin 18 °C) in a two-dimensional horizontal annulus heated by two discrete heat sources attached at the inner cylinder keeping the rest of walls insulated. They examined the effect of heat sources arrangement on melting process. It was indicated that heat sources location on the bottom part show higher rate of melting.

From the previous literature, it was shown that most of studies on PCM with discrete heat sources have been restricted to geometric parameters evaluation such as heat source arrangement, size, length, spacing and enclosure aspect ratio. To the best knowledge of the authors, the manner of arranging different power component and intermittent regime are not yet been reported. Therefore, the focus of this paper is to investigate experimentally the melting process of a PCM in a rectangular enclosure with three discrete heat sources. In order to get closer to real applications and optimize the source emplacement, the effect of heat flux repartition between sources and intermittent periodic heat flux is evaluated on cooling performance of system based primarily on maximizing the critical time.

2. Experimental apparatus and procedure

The schematic diagram of the apparatus used in this study is shown in Fig. 1(a). It consists mainly of a PCM container with three discrete sources, a power supply, a temperature data logger, a personal computer and a digital camera.

Fig. 1(b) shows the schematic representation of the cooling system. This system consists of a rectangular cooling system with the inner dimensions of 170 mm (height), 58 mm (width) and 243 mm (depth). The discretely heated right vertical wall of the enclosure was made of Bakelite with (thickness = 10 mm). Three identical $(20 * 243)\,mm^2$ equidistant (20 mm) electric resistances were attached below copper plate with the same dimensions on the substrate of Bakelite and joined to a power supply (Sorensen XFR 150-18). The other walls of the enclosure were made of 20 mm thick (top and bottom faces), 10 mm thick (left, front and rear faces) of transparent Plexiglas sheets to allow for the photographic observation of the melting process. For further insulation, the enclosure was insulated with polystyrene. The PCM used in this study was a commercial product, Plastic paraffin. Thermal properties of PCM are reported below in Table 1. An air layer of 10 mm thickness was provided in the top of cavity for PCM expansion during the melting. The experiments were performed by monitoring reading of thermocouples on the discretely heated vertical wall for 200 min. The vertical position is adopted for this study.

Twenty-one thermocouples with a calibrated accuracy of ±0.5 °C were differently distributed at the same section (located 50 mm from the rear face) shown in Fig. 2 to measure the transient temperature distribution. This section included three units: one at the inner right wall and two others placed in PCM respectively at x_1 = 19 mm and x_2 = 39 mm away from the source plate. The two latter units were served to confirm the melting front position. All thermocouples are connected to the computer through a data logger (KEITHLEY 3706) to record temperature. A digital camera (Nikon D90) was used to visually record the melting front evolution every 10 min. The temperatures of the PCM at the specified locations were logged every 10 s. Each experiment was performed twice to verify their repeatability. The experiments were conducted at an ambient temperature of (19 °C ± 1 °C).

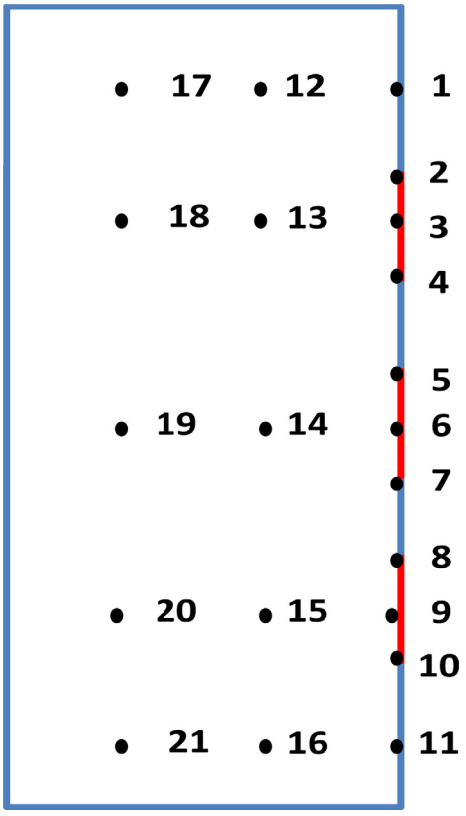

Fig. 2. Schematic representation of thermocouples locations.

3. Mathematical model

The heat transfer and fluid flow analysis in the cooling system are assumed to be two-dimensional. The flow of the molten PCM in heat sink assumed to be laminar, incompressible. The PCM is supposed to be pure, homogenous and with isotropic physical properties. The governing equations used here for the PCM are:

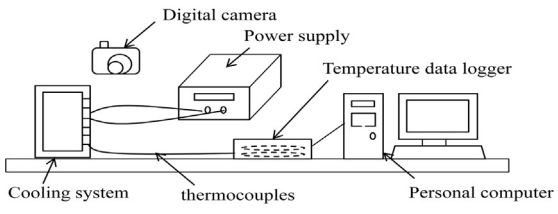

(a)

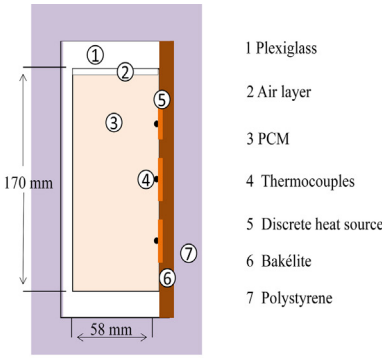

(b)

Fig. 1. (a) Schematic diagram of the experimental apparatus. (b) Schematic representation of cooling system.

Table 1
Thermo-physical properties of PCM.

Materials	Thermal conductivity k ($W\,m^{-1}\,K^{-1}$)	Specific heat capacity C_p ($kJ\,kg^{-1}\,K^{-1}$)	Density ρ ($kg\,m^{-3}$)	Melting temperature T_m (°C)	Latent heat L_m (kJ/kg)
Plastic paraffin	0.234(s) 0.164(l)	2.710(s) (25 °C) 4.640(l) (65 °C)	900(s) 770(l)	51.75	138.23

Momentum equations

$$\rho_l\left(\frac{\partial u}{\partial t}+U\frac{\partial u}{\partial x}+V\frac{\partial u}{\partial y}\right)=-\frac{\partial P}{\partial x}+\mu_l\left(\frac{\partial^2 u}{\partial x^2}+\frac{\partial^2 u}{\partial y^2}\right)+Bu \quad (1)$$

$$\rho_l\left(\frac{\partial v}{\partial t}+U\frac{\partial v}{\partial x}+V\frac{\partial v}{\partial y}\right)=-\frac{\partial P}{\partial x}+\mu_l\left(\frac{\partial^2 v}{\partial x^2}+\frac{\partial^2 v}{\partial y^2}\right)+\rho_0 g\beta(T-T_0)+Bv \quad (2)$$

The thermal expansion coefficient, β, is introduced into the momentum Eq. (2) to include the buoyancy force term, according to the Boussinesq's approximation:

$$\rho=\rho_0 g\beta(T-T_0) \quad (3)$$

H_l is the liquid fraction during the phase change which is defined by the following relations:

$$H_l=0 \quad \text{if } T\prec T_m \quad (4)$$

$$H_l=1 \quad \text{if } T\succ T_m \quad (5)$$

The momentum source terms Bu and Bv (Eqs. (1) and (2)) were used for cancel velocities in solid region where $B(H_l)$ is the porosity function:

$$B=\frac{-C\left(1-H_l^2\right)}{\left(H_l^3+b\right)} \quad (6)$$

where b is a small computational constant used to avoid division by zero, and C is a constant reflecting the morphology of the melting front.

Energy equation

$$Cp_{eq}\frac{\partial T}{\partial t}=\lambda_{eq}\left(\frac{\partial^2 T}{\partial x^2}+\frac{\partial^2 T}{\partial y^2}\right)-Cp_{eq}\left(u\frac{\partial T}{\partial x}+v\frac{\partial T}{\partial y}\right) \quad (7)$$

where Cp_{eq} and λ_{eq} represent respectively the equivalent volume heat capacity and equivalent thermal conductivity.

$$Cp_{eq}=H_l(\rho Cp)_l+(1-H_l)(\rho Cp)_s \quad (8)$$

$$\lambda_{eq}=H_l\lambda_l+(1-H_l)\lambda_s \quad (9)$$

The governing equations previously described are solved using COMSOL MULTIPHYSICS. This code uses discretization and a formulation based on the finite element method.

4. Results and discussion

The numerical model has been validated with experimental results. Fig. 2 shows the comparison of the melting front position at two different instant between experimental (Fig. 3(a)) and numerical work (Fig. 3(a)). It was observed that there is a slight difference between both results.

As mentioned above, the behavior of PCM with discrete heat sources is investigated in this paper. The selection of the heat repartition effect is in view that electronic devices generate frequently different heat dissipation rates. Also, this parametric study allows identifying the configuration ensuring the long and safe system operation. For all cases, the total heat flux input remains constant. The critical time t_c is selected as a heuristic parameter for the reason of comparison between various configurations performance. It is defined as the time before at least one heat source achieves the critical temperature of electronics.

As shown in Table 2, ten different cases are studied: Case 1 is the reference case where the total heat is uniformly distributed between sources, case 2, 3 and 4 where the total heat is concentrated respectively at the upper, middle and lower source and case 5–10 where the total heat is non-uniformly distributed between sources. Q_1, Q_2 and Q_3 represent respectively the heat flux imposed at the upper, middle and lower source and the total heat flux is equal to 9000 W m^{-2}.

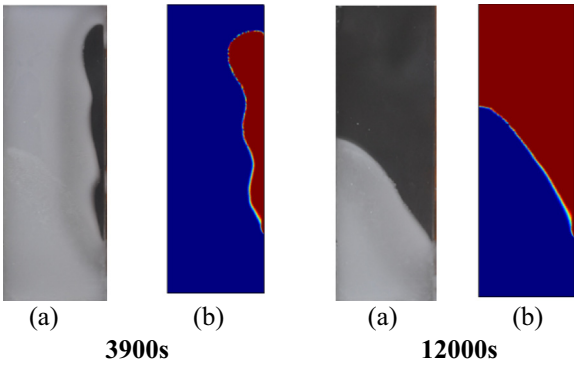

Fig. 3. Comparison of the melting front position at two instants between experimental (b) and numerical (a) results.

4.1. Effect of uniform repartition of heat flux (case 1)

4.1.1. Photographic observation of melting front evolution

The knowledge of the heat transfer mechanism during melting is essential to the understanding of phenomenon. Therefore, in Fig. 4(i) the melting front position at various times of 1200, 2100, 3900, 6300, 9600 and 12,000 s are depicted. In these photographs, the black and white colors observed represent respectively the liquid and solid phases. At early time (t = 1200 s), it can be noticed the formation of three equal thin layers of liquid PCM near their respective heat sources. At time = 2100 s, convection establishes resulting the interface distortion at the high level of each liquid area. As time progresses, the three liquid zones are rapidly merged to form one liquid region. The buoyancy is developed; consequently, the solid-liquid interface is more advanced near the upper region of the cavity. After (t = 12,000 s), the majority of PCM is melted, whereas a weaker part of PCM remains in the bottom region. In order to confirm the melting front position, a comparison of melting front position between the digital photograph (a) and the interpolated temperature result (b) is presented at the same instant (9600 s) in Fig. 4(ii). The interpolation is done between temperatures at different emplacements. The identification of the melting front is based on melting temperature determination. It was seen that there is not a difference between both photos.

4.1.2. Variation of the surface temperature of heat sources

Fig. 5 presents the temporal evolution of heat source temperature. T_{H1}, T_{H2} and T_{H3} indicate respectively the average temperature at the upper (between thermocouples 1, 2 and 3), middle (between thermocouples 4, 5 and 6) and lower heat source (between thermocouples 7, 8 and 9) shown in Fig. 2. In Fig. 5, we can see at first the same temperature profile for three sources. At the beginning, the temperature increases rapidly and this is similarly observed for all sources. This phase corresponds to the conduction regime. Then, we can notice a plateau for all sources which can be explained by the melting onset and convective regime establishment in each liquid area (Fig. 5(instant a)). Afterwards, we can remark a re-increase of temperature expect for the inferior source and a higher slope for the upper source. This is due to the junction of three liquid zones (Fig. 5(instant b)) causing the ascension of the hot liquid PCM from the inferior source to sources above. Then, a steady state was shown due to the convection development in liquid region (Fig. 5(instant c)) and its capacity to transport the total heat supplied to the solid PCM. Finally,

Table 2
Different cases of heat flux repartition.

Case	1	2	3	4	5	6	7	8	9	10
Q_1 (W m^{-2})	3000	9000	0	0	4500	4500	0	5000	2000	2000
Q_2 (W m^{-2})	3000	0	9000	0	4500	0	4500	2000	5000	2000
Q_3 (W m^{-2})	3000	0	0	9000	0	4500	4500	2000	2000	5000

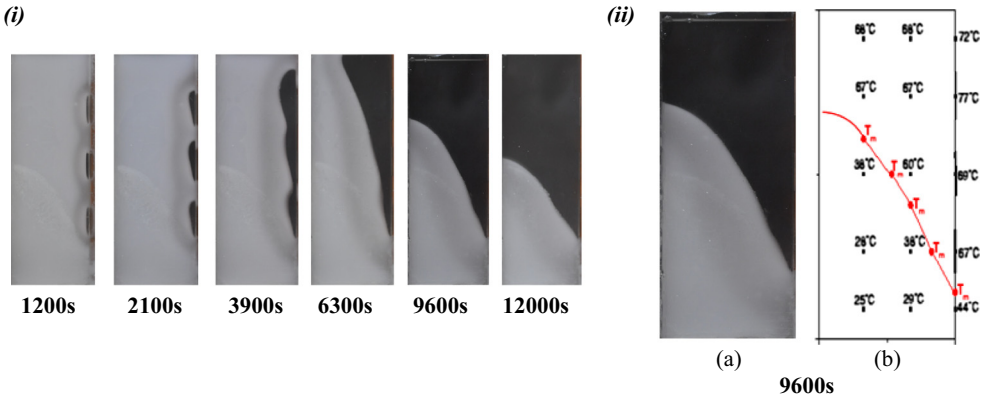

Fig. 4. (i) Experimental melting front position at various times for case 1 and (ii) comparison of melting front position at instant 9600 s between the digital photo and interpolation result.

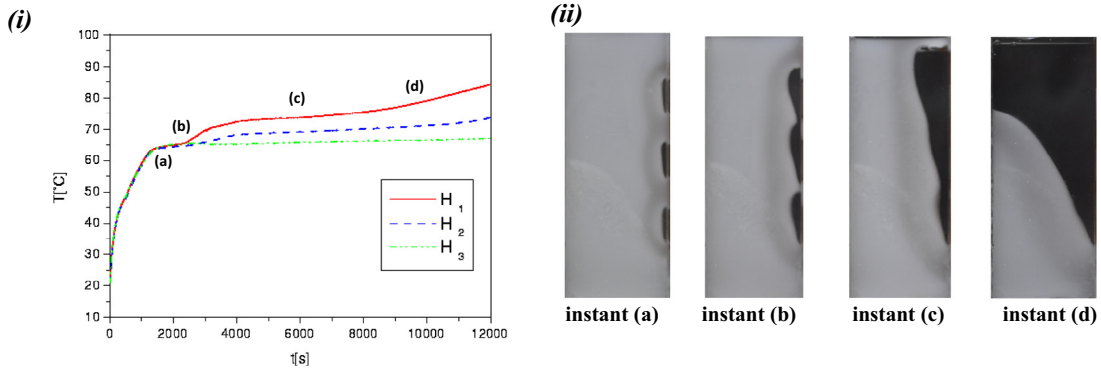

Fig. 5. (i) Variation of temperature of the three heat sources for the case 1 and (ii) photographs of melting front at different times.

once melted the PCM placed in front of each source, the steady state was leaved first by the upper (Fig. 5(instant d)) then the central source. Whereas, this trend is not yet seen for the lower source. To conclude, it can be said for this configuration that the maximum temperature is detected at the higher component because of the thermal interaction from components below, while the minimum temperature is noted at the bottom component.

4.2. Effect of heat flux concentration (case 2, 3 and 4)

The best manner to arrange a high power component can extend the critical time of system for many applications. So, the location effect of the heat flux on the thermal performance will be discussed in this part. In order to do this, the total heat flux is concentrated first at the upper (case 2) then at the middle (case 3) and finally at the lower heat source (case 4) maintaining every time the others sources deactivated. In Fig. 6 the time variations of the source temperature (i) and liquid fraction (ii) are displayed for different heat flux concentration corresponding to cases 2, 3 and 4. This figure shows that the temperature variation goes through three distinct regions. At the earlier stage, the conduction regime predominates leading to a great increase in temperature. After this stage, it is noticed a plateau of temperature which is explained as early by the melting onset of PCM and the convection development in liquid. The plateau presents an ascendant length from the upper to the lower heat location. This can be due to the importance of solid PCM amount placed above the heat source in promoting convection. For liquid fraction, a linearly increase is remarked during this period for all cases. Finally, a re-increase of temperature was seen for the two cases (2 and 3) except for case 4. Here a slope decays is seen as an equivalent observation for liquid fraction. The reason behind this slope change is the heat transfer weakness caused by the full melting of PCM placed in front of source and moving down of the interface as shown in (Fig. 7 (instant a and b)). While for case 4 there stills yet a solid PCM as shown (Fig. 7(instant c)). Although in three cases the temperature reaches high values in short times, arranging a higher power component at the lower location is seen more efficient for such applications.

4.3. Effect of non-uniform repartition of heat flux

Practically, electronic components might generate different power. Therefore, in this part non-uniformly distribution of heat flux corresponding to case 5 to case 10 is investigated.

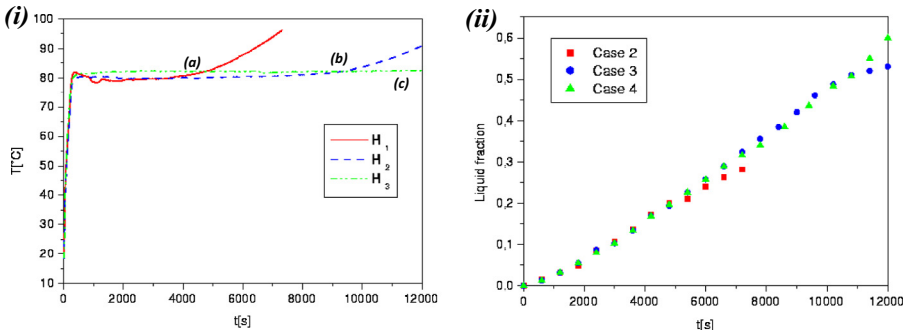

Fig. 6. Variation of (i) temperature (ii) liquid fraction of the three heat sources for the three cases (2, 3 and 4).

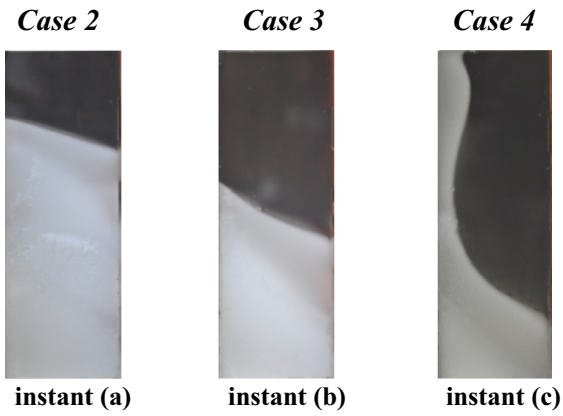

Fig. 7. Photographs of the melting front of different flux concentration at different instants (a, b and c).

4.3.1. Two heat sources activated (case 5, 6 and 7)

In this section, the heat flux is differently partitioned between two heat sources. Fig. 8 presents the temperature variation of heat sources with time for three cases (5, 6 and 7). As it can be seen, for all cases nearly the same temperature profile is noticed. First, all cases show superposed temperature noting the conductive phase. Second, a plateau of superposed temperature is observed which lasts around 900 s for cases (5 and 7) while it extends to 4700 s for case 6. The plateau's length can be interpreted by the time elapsed by the two liquid regions to join each others as shown in Fig. 9(instant a, c and e). Afterward, as seen before, once merged the liquid regions, the hot liquid ascends and causes an increase of the superior source temperature. Then, it is clearly remarked a constant temperature for cases 5 and 7 except for case 6. We can explain this pattern by the fact that in case 6 an important amount of PCM was already melted before the junction of the two liquid regions (Fig. 9(instant c)). Later, this temperature rises in case 5 while it is kept constant for case 7. This can be explained respectively by the existence of solid PCM above sources as indicated in (Fig. 9(instant f)) and the full melting of PCM in front of source as seen in (Fig. 9(instant b)). Finally, we can conclude that dividing heat flux between middle and lower source has the best efficiency for applications with long operating time. Whereas, for applications with short operating time, it is advantageous to partition heat flux between the farther sources (activating the upper and lower source).

4.3.2. Three heat sources activated (case 8, 9 and 10)

In this part, different heat flux repartitions between the three sources are studied. In Fig. 10, the temperature variation of heat sources with time for three cases (8, 9 and10) are presented. In order to simplify the interpretation process, the source generating the great part of heat flux (5000 W m^{-2}) is noted H_{gr} while that generating the weaker is designed by the notation H_w. For all cases, it can be seen that at early stages, the conductive phase is similar for two sources H_w while it presents a higher slope for H_{gr}. It is important to note that the temperature of source H_{gr} reaches rapidly the permanent regime indicating around 70 °C for all cases. Afterwards, this temperature notes a clearly rise in case 8 and a slight one in case 9 while for the case 10 it remains stable. The fact that the PCM is fully melted in front of each source shown in Fig. 11 (instant b and d) while it stills solid for case 10 (Fig. 11(instant f)) can justify this trend. Concerning the two sources H_w, since two liquid regions merged with each others, the source placed above receive the hot liquid then indicates a temperature rise illustrated in Fig. 11(instant a, c and e). After that, it finishes finally by catching up the H_{gr} temperature in case 9, remaining stable in case 8 and order inversing with the second source H_w in case 10. It can be concluded from this part that placing the higher part of heat flux in

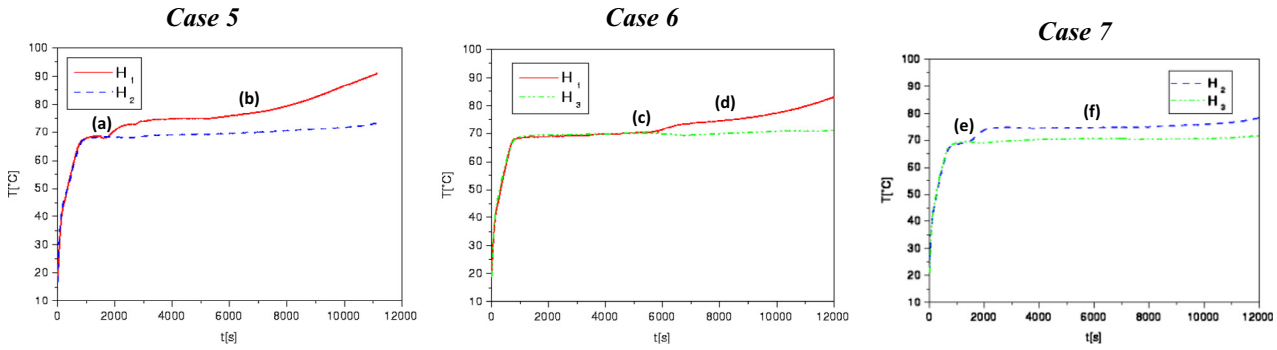

Fig. 8. Variation of temperature of heat sources versus time for the three cases (5, 6 and 7).

DOI : 10.1016/j.applthermaleng.2016.06.109

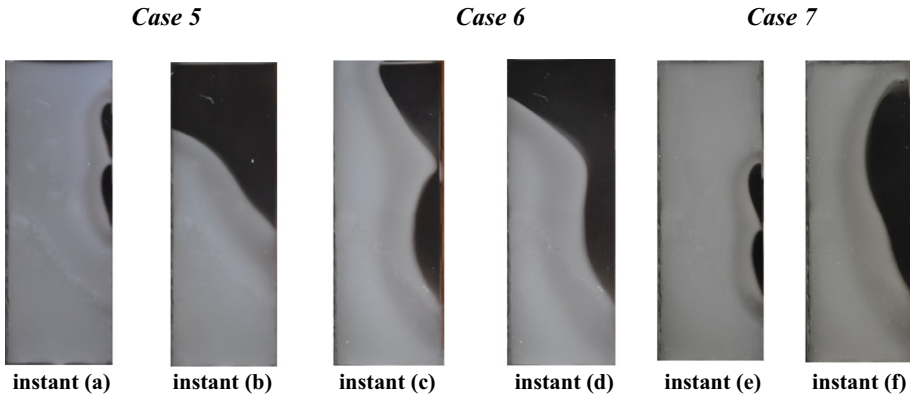

Fig. 9. Photographs of the melting front of different flux repartition (case 5, 6 and 7) at different times.

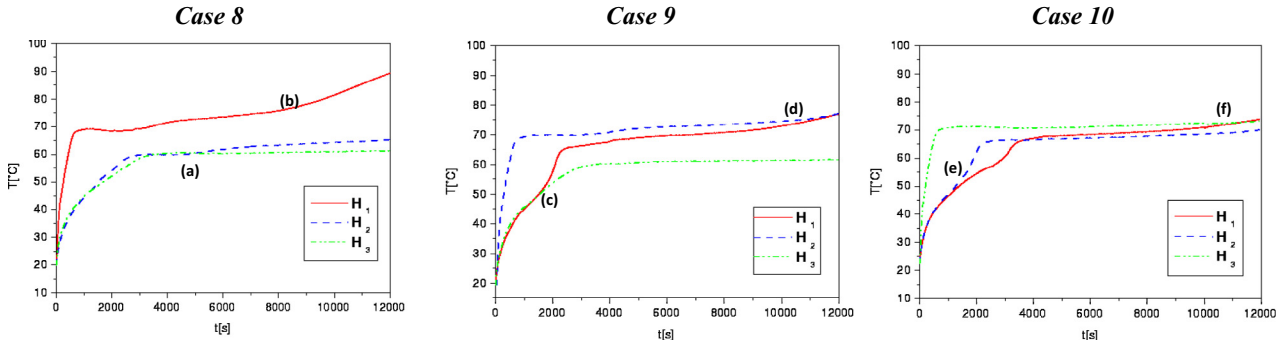

Fig. 10. Variation of temperature of heat sources versus time for the three cases (8, 9 and 10).

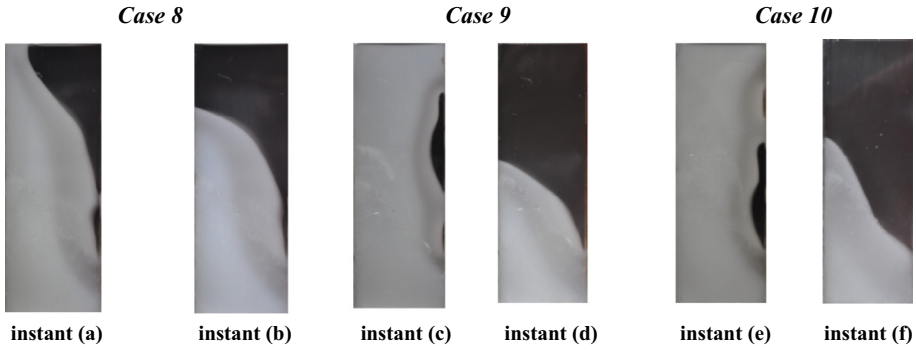

Fig. 11. Photographs of the melting front of different flux repartition (case 8, 9 and 10) at different times.

middle or lower source shows an interesting contribution to stabilize longer the critical temperature, whereas imposing it at the upper location leads rapidly to the overheating.

4.4. Comparison of critical time

Maintaining the heat source below a critical temperature for a long time represents a crucial challenge for several industrial applications. Therefore, the different configurations are compared in Fig. 12 by exhibiting the critical time elapsed to reach the critical temperature (77 °C) for all cases except case 2, 3 and 4. These three configurations are not depicted seeing that their critical time is notably low. The case 1 is considered as a reference configuration. The shaded area seen in this figure for case 10 represents the continuation of critical time extending even after 200 min. It can be seen first that although the reference case presents a favorable critical time (150 min), there are more important ones (173, 188, 199

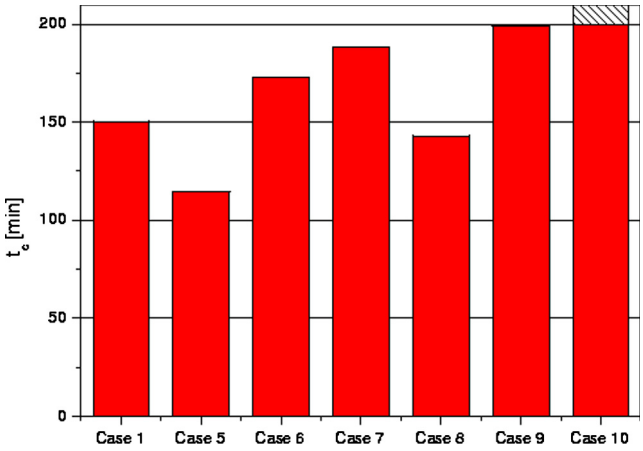

Fig. 12. Comparison of the critical time for different repartition cases.

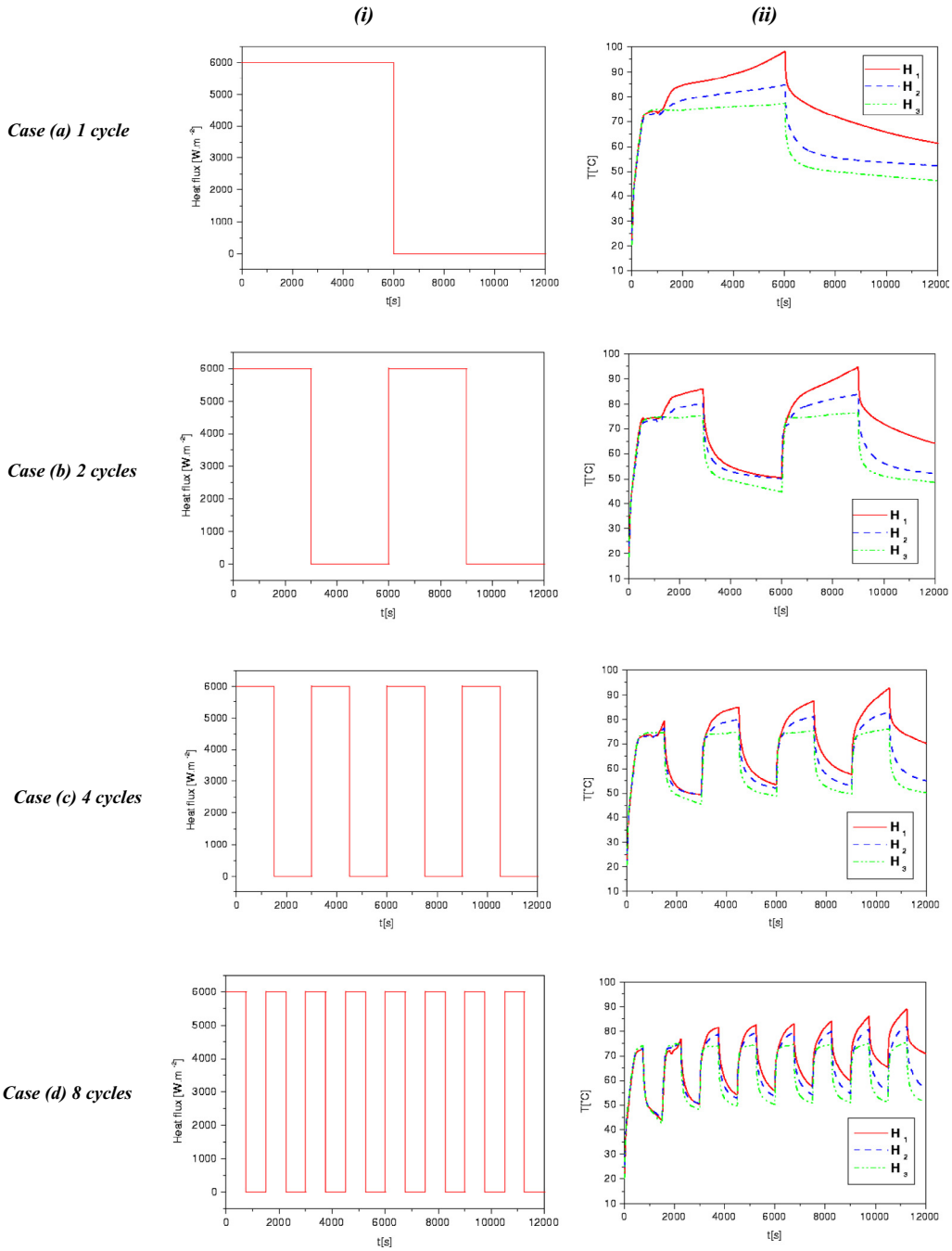

Fig. 13. Different cyclic heat fluxes and variation of temperature of the three heat sources versus time.

and even more than 200 min) respectively for the cases (6, 7, 9 and 10). It is noticed that the lowest efficiency seen correspond to the case 5 and 8 when the great part of heat flux was imposed at the upper source. It can be concluded that the great part of heat flux should be imposed at the lower source while the upper should be either deactivated or submitted to a weak part of heat flux.

4.5. Effect of intermittent regime

In order to get closer to real applications, the intermittent cyclic regime was selected to be examined in this part.

Therefore, the permanent heat flux (F amplitude) has been replaced by a periodic cycle (on/off) with a double amplitude ($2 * F$) for the same operating time. Next, the cycle number was multiplied by (2, 4 and 8) conserving the same operating time by reducing every time the period length. Fig. 13(i) represents the different intermittent regimes studied. For all cases, the cycle includes two equal phases: a switch on phase followed by a switch off one. The heat flux is equal to 6000 W m^{-2} per source.

The temporal behaviors of the temperature at each source for all intermittent regimes were presented in Fig. 13(ii). First, it is clearly observed the synchronization of thermal response with the heat flux input for all cases. During the phase of (switch on), it is remarked that the temperature amplitude of H_1 increases over cycles for all cases. Once natural convection is established, this temperature keeps notably the same amplitude for respectively two and five successive cycles in cases (c) and (d). This pattern can be explained by the fact that fractionate the period length into

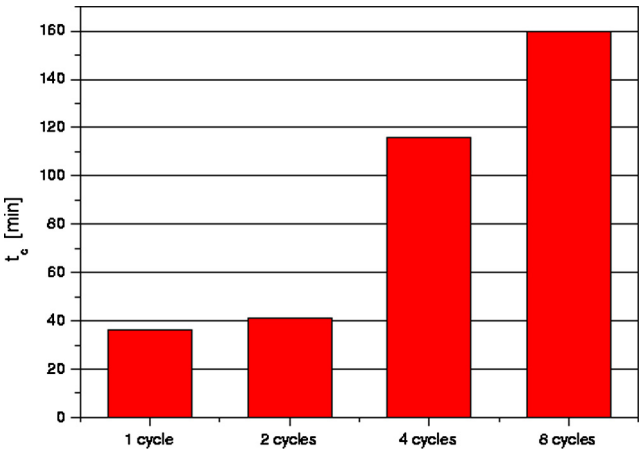

Fig. 14. Comparison of the critical time for different cycle number.

4 and 8 cycles leads to intensify the phase of switch off and keep by consequent the PCM in front of the upper source not fully melted. During the switch off phase, it is important to note that the temperature of H_1 presents a lower slope comparing to the two sources below intensifying over cycles. By turning our focus to the others heat sources H_2 and H_3; it is clearly noticed a stable pattern of their temperature amplitude during cycles for the two phases. Comparing all cases, it is clearly distinguished that fractionating cycle period affects positively the temperature stabilization.

In this part, as seen the heat flux imposed is doubled to simulate the high power electronic components. Therefore, the critical temperature selected is 85 °C. In order to quantify the effect of different cycle number on thermal performance, the critical time elapsed below reaching this limit temperature is compared for different cycle number in Fig. 14. First, an extension of the critical time is observed with cycle number. Therefore, it increases slightly (around 5 min) from 1 to 2 cycles. While fractionating the cycle length into 4 and 8 shows a significant performance to extend the critical time respectively more than 3 time and nearly 5 times comparing to 1 cycle. It can be concluded that increasing the cycle number conserving the same time working offers a longer period of safe operation.

5. Conclusions and future works

An experimental study has been presented to determine experimentally an efficient configuration controlling three heat sources by a single vertical rectangular enclosure filled with a phase change material. Different manners to distribute heat flux between sources are examined: the concentration of the total heat flux, the uniform and no uniform repartition of heat flux between sources. The PCM behavior for different cases is explored to better understand the mechanism of heat transfer. Then to get closer to real application, the intermittent regime is studied and discussed for different cycle number. From the results it has been found that:

- For the uniform distribution of heat flux, the maximum temperature is detected at the higher component while the minimum is at the bottom one.
- The best efficient arrangement of a higher power component is at the lower location.
- Dividing heat flux equally between middle and lower source seems suitable for applications with long operating time.
- Partitioning heat flux between the two farther sources shows advantage for applications with short operating time.
- Placing the great part of heat flux in middle or lower source seems an interesting contribution to maintain longer safe the component.
- Fractionate cycle length into 4 or 8 cycles conserving the time working, extends respectively nearly 3 and even 5 times the critical time comparing to one cycle.

To improve the efficiency of these systems, future work could explore:

- The opportunity of adding fins by testing the better method: separate fins of each heat source or common for the three heat sources.
- The system behavior in the case when the three sources operated alternately.
- Higher critical temperature to simulate other applications.

References

[1] R. Kandasamy, X. Wang, A.S. Mujumdar, Application of phase change materials in thermal management of electronics, Appl. Therm. Eng. 27 (2007) 2822–2832.
[2] F.L. Tan, C.P. Tso, Cooling of mobile electronic devices using phase change materials, Appl. Therm. Eng. 24 (2004) 159–169.
[3] M. Faraji, H. El Qarnia, Numerical optimization of a thermal performance of a phase change material based heat sink, Int. J. Heat Technol. 26 (2) (2008) 17–24.
[4] S. Gharbi, S. Harmand, S. Ben Jabrallah, Experimental comparison between different configurations of PCM based heat sinks for cooling electronic components, Appl. Therm. Eng. 87 (2015) 454–462.
[5] K. Keyhani, V. Prasad, R. Cox, An experimental study of natural convection in a vertical cavity with discrete heat sources, ASMEJ Heat Transf. 110 (1988) 616–624.
[6] M.L. Chadwick, B.W. Webb, H.S. Heaton, Natural convection from two-dimensional discrete heat sources in a rectangular enclosure, Int. J. Heat Mass Transf. 34 (1991) 1679–1693.
[7] Y. Liu, N. Phan-Thien, An optimum spacing problem for three chips mounted on a vertical substrate in an enclosure, Numer. Heat Transf. Part A 37 (2000) 613–630.
[8] Phani Krishna Kadiyala, Himadri Chattopadhyay, Optimal location of three heat sources on the wall of a square cavity using genetic algorithms integrated with artificial neural networks, Int. Commun. Heat Mass Transf. 38 (2011) 620–624.
[9] Qi-Hong Deng, Guang-Fa Tang, Yuguo Li, Man Yeong Ha, Interaction between discrete heat sources in horizontal natural convection enclosures, Int. J. Heat Mass Transf. 45 (2002) 5117–5132.
[10] T. Basak, S. Roy, A.R. Balakrishnan, Effects of thermal boundary conditions on natural convection flows within a square cavity, Int. J. Heat Mass Transf. 49 (2006) 4525–4535.
[11] B. Binet, Étude de la fusion dans des enceintes munies de sources de chaleur discrètes, Thèse de Doctorat, Sherbrooke (Québec), Canada, 1998.
[12] Z. Jianhua, C. Zhongqi, L. Dengying, L. Ji, Experimental study on melting in a rectangular enclosure heated below with discrete heat sources, Int. J. Therm. Sci. 10 (2001) 254–259.
[13] Y. Zhang, Z. Chen, Q. Wang, Q. Wu, Melting in an enclosure with discrete heating at a constant rate, Exp. Therm. Fluid Sci. 6 (1993) 196–220.
[14] M. Faraji, H. El Qarnia, Numerical study of melting in an enclosure with discrete protruding heat sources, Appl. Math. Model. 34 (2010) 1258–1275.
[15] H. El Qarnia, A. Draoui, E.K. Lakhal, Computation of melting with natural convection inside a rectangular enclosure heated by discrete protruding heat sources, Appl. Math. Model. 37 (2013) 3968–3981.
[16] H. Mirzaei, A. Dadvand, M. Mastiani, S. Sebti, S. Kashani, Melting of a phase change material in a horizontal annulus with discrete heat sources, Therm. Sci. 19 (2015) 1733–1745.